J. DIFERENSIAL/E-ISSN:2775-9644
Vol.8(2),2026, 120–135
doi:https://doi.org/10.35508/jd.v8i2.27037

RESEARCH ARTICLE

Modeling the Impact of Mint Leaf Therapy and Sanitation on Malaria Transmission among Infants

Babatunde O. Awominure[1,*], Amos O. Popoola[1], Tosin Oreyeni[1]

[1]*Faculty of Basic and Applied Sciences, Department of Mathematical Sciences, Osun State University, Nigeria*
[*]*Corresponding author: awominuretunde@gmail.com*

Received: 15 January 2026; Revised: 20 February 2026; Accepted: 10 April 2026; Published: 1 September 2026.

Abstract:
Malaria transmission among infants remains a persistent concern to health care practitioners in regions with this disease equilibrium, motivated by the assessment of complementary intervention alongside conventional treatment strategies can help submerge this prevalence. This study investigate the combined effects of mint leaf (*Mentha piperita*) herbal therapy and environmental hygiene on malaria dynamics within infant population. The human population is partitioned into susceptible, exposed, infectious, mint treated and recovered compartments, while the vector dynamics are represented by the infected mosquito population. To enhance epidemiological realism, mosquito-to-human transmission is described by a linear saturated force of infection that incorporates sanitation effects and restricts unbounded growth of infection pressure at elevated vector densities. Two time-dependent control functions are embedded in the model: mint leaf therapy, which augments treatment and recovery rates and sanitation measures, which attenuate bidirectional transmission between humans and mosquitoes. The model further incorporates newborn recruitment, inflow of infected infants, natural mortality, waning immunity and mosquito population turnover. Qualitative analysis confirms the well-possedness of the model by establishing positivity and boundedness of solutions within a positively invariant region. Numerical simulation was carried out using the Laplace adomian decomposition method to demonstrate the effectiveness of the control measures. Simulation results has a significant reduction in infectious infants and infected mosquitoes under enhanced herbal treatment and sanitation coverage. This model provides a robust means to evaluate malaria control strategies through mint leaf and offers a foundation for further stability, sensitivity and optimal control analysis of this therapy.

Keywords: Malaria, Mint leaf herbal therapy, Environmental hygiene, Vector–host dynamics, Infant population.

1. Introduction

Malaria persists a public health burden among infants in endemic regions, characterized by sustained transmission driven by the nonlinear interaction dynamics between the human host population and the mosquito vector population [1]. Despite the availability of conventional antimalarial

drugs, limitations such as drug resistance, limited access to healthcare, and poor environmental sanitation continue to hinder effective disease control [2]. Consequently, there is increasing interest in complementary and community-based interventions, including herbal therapies and improved hygiene practices, as supportive strategies for malaria reduction [3].

This study modifies a deterministic compartmental model which was develop to investigate the combined effects of mint leaf (*Mentha piperita*) herbal therapy and environmental hygiene on malaria transmission dynamics among infants. The human population is stratified into susceptible, exposed, infectious, mint-treated, and recovered compartments, while the vector population is represented by infected mosquitoes. This structure enables the model to capture the natural progression of malaria infection from exposure to treatment and recovery, as well as the possibility of waning immunity and reinfection [4].

Two time-dependent control functions are incorporated into the model. The first represents the coverage of mint leaf herbal therapy, which enhances treatment and recovery rates among infected infants. The second control captures sanitation and environmental hygiene efforts, which reduce mosquito human contact and limit mosquito infection from humans [5].

To ensure biological realism, the mosquito-to-human force of infection is modeled using a linear saturated incidence function. This formulation prevents unbounded growth of infection pressure at high mosquito densities and reflects realistic constraints on transmission intensity under improved environmental conditions. The model further accounts for the recruitment of newborn infants, inflow of infected infants, natural mortality, and mosquito population dynamics [6, 7].

By integrating herbal treatment and sanitation within a unified mathematical model. malaria model provides insight into the potential effectiveness of alternative and supportive malaria control strategies [8]. The system is shown to be well-posed and biologically meaningful within a positively invariant region, forming a solid basis for subsequent analytical and numerical investigations of malaria control under combined intervention measures [9].

To accomplish this, it is necessary to acquire the model solution. However, given the absence of an exact solution for the model, we will employ distinct numerical approximation schemes of the Laplace Adomian Decomposition Method to determine an accurate and precise approximate solution for the model [10].

2. Materials and Method

2.1. Formulation of Model

The human population is divided into susceptible, exposed, infectious, mint-treated (*Mentha piperita*) individuals $M(t)$ and recovered $R(t)$ compartments, while $V(t)$ represents the infected mosquito population. Two control mechanisms are incorporated: mint-leaf herbal treatment $\phi_1(t)$ and sanitation/environmental hygiene $\phi_2(t)$.

Transmission from mosquitoes to infants is modeled using a linear saturated force of infection as described in Table 2.1 and Equation (1) below. The model equations are defined in Equation (2) respectively.

Table 2.1: Parameters description, values and references

Parameters	Description	Values	References
$S(t)$	Susceptible population		
$E(t)$	Exposed population	7600	[6]
$I(t)$	Infected population	1022	[3]
$M(t)$	Mint treated (*Mentha piperita*) population	903	[1]
$R(t)$	Recovered population	1682	[2, 4]
$V(t)$	Infected mosquito population	348	[6]
Λ	Recruitment rate of newborn infants into susceptible population	0.113	[1, 8]
p	Fraction of infants given mint treatment at entry	0.015	[7]
$\mathcal{A}$	Number of infants arriving with malaria infection	1.0126	[2]
μ	Natural mortality rate	0.182	[1]
δ	Rate of loss of immunity (returning R to S)	0.124	[8]
β	Baseline mosquito to human transmission rate	0.253	[6]
η	Direct exposure rate of susceptible	0.4	[3]
σ	Rate at which exposed infants progress to infection	0.001	[7]
τ	Clinical treatment rate for infected infants	0.5	[5]
κ	Additional treatment rate due to mint therapy	0.2	[2, 5]
ω	Recovery rate due to mint (herbal treatment) efficacy	0.03	[4]
α	Human-to-mosquito transmission rate	1.0	[6]
ϕ_v	Recruitment rate of infected mosquitoes	0.016	[1]
μ_v	Natural death rate of mosquito	0.113	[7]
γ_v	Additional mosquito removal rate	1.0126	[2]
N_v	Total mosquito population (scaling factor)	0.12	[3]
χ_1	Sanitation effectiveness on mosquito-to-human transmission	0.124	[1]
χ_2	Sanitation effectiveness on human-to-mosquito transmission	0.21	[1]
ϕ_1	Control variable for mint-leaf treatment coverage	0.02	[6]
ϕ_2	Control variable for sanitation	0.14	[2, 7]
$\Lambda_{\max}$	Maximum saturation level of force of infection	0.23	[7]

$$M(t) = \min\left(\beta(1-\chi_2\phi_2)\frac{V(t)}{N_v}, \Lambda_{\max}(1-\chi_2\phi_2)\right) \tag{2.1}$$

which ensures that infection pressure does not grow unbounded. The model captures malaria infection progression through exposure, infection, treatment and recovery, while accounting for the impact of mint leaf therapy and improved sanitation on disease reduction. The system is well posed within a positively invariant region [6]. From the saturated force of infection as indicated above in equation 2.1, it is obtained for equation 2.2 below the model equation denoting the transmission and coherence of the populations as said above.

$$\begin{aligned}
S^1 &= \Lambda + (1-p)\Lambda + \delta R - \lambda(t)S - (\mu+\eta)S \\
E^1 &= \lambda(t)S + \eta S - (\mu+\sigma)E \\
I^1 &= \sigma E - (\mu+\tau+\kappa\phi_1)I \\
M^1 &= p\Lambda + (\tau+\kappa\phi_1)I - (\mu+\omega)M \\
R^1 &= \omega M - (\delta+\mu)R \\
V^1 &= \varphi_v - (\mu_v+\gamma_v)V + \alpha(1-\chi_2\phi_2)I
\end{aligned} \tag{2.2}$$

Where the saturated force of infection is defined as above and its initial conditions are subjected

$$S(0) = s_0, \quad E(0) = e_0, \quad I(0) = i_0, \quad M(0) = m_0, \quad R(0) = r_0, \quad V(0) = v_0 \geq 0.$$

2.2. Existence and Uniqueness of Model Solution

Hence, the solutions of system of equation (2) are bounded if we consider the total population. The variation in the total population concerning time is given by:

$$N(t) = S(t) + E(t) + I(t) + M(t) + R(t) + V(t)$$

Considering this to the total population $N(t)$ at time t which is given by,

$$\frac{dN(t)}{dt} = \frac{d}{dt}\left(S(t) + E(t) + I(t) + M(t) + R(t) + V(t)\right) \tag{2.3}$$

Substituting the respective compartments in equation 2.3 above yields;

$$\begin{aligned}
S^1 &= \Lambda + (1-p)\Lambda + \delta R - \lambda(t)S - (\mu+\eta)S \\
E^1 &= \lambda(t)S + \eta S - (\mu+\sigma)E \\
I^1 &= \sigma E - (\mu+\tau+\kappa\phi_1)I \\
M^1 &= p\Lambda + (\tau+\kappa\phi_1)I - (\mu+\omega)M \\
R^1 &= \omega M - (\delta+\mu)R \\
V^1 &= \phi_v - (\mu_v+\gamma_v)V + \alpha(1-\chi_2\phi_2)I \\
N^1(t) &\leq [\,\Lambda + (1-p)\Lambda + \delta R - \lambda(t)S - (\mu+\eta)S\,] + [\,\lambda(t)S + \eta S - (\mu+\sigma)E\,] \\
&+ [\,\sigma E - (\mu+\tau+\kappa\phi_1)I\,] + [\,p\Lambda + (\tau+\kappa\phi_1)I - (\mu+\omega)M\,] \\
&+ [\,\omega M - (\delta+\mu)R] + [\,\phi_v - (\mu_v+\gamma_v)V + \alpha(1-\chi_2\phi_2)I\,]
\end{aligned}$$

$N^1(t) + \mu N \leq \Lambda$, resolving this by the technique of integrating factor for a differential equation at time $t = 0,\ c = N(0) - \frac{\Lambda}{\mu}$ where c is the constant of integration. Hence, it is obtained that $N^1(t)$, on the total population $N(t)$, progressively yields:

$$\lim_{t\to\infty} N(t) \leq \lim_{t\to\infty}\left[\frac{\Lambda}{\mu} + \left(N(0) - \frac{\Lambda}{\mu}\right)e^{-\mu t}\right] = \frac{\Lambda}{\mu} \tag{2.4}$$

Then $N(0) \leq \frac{\Lambda}{\mu}$, then $N(t) \leq \frac{\Lambda}{\mu}$. This is sufficient to consider the dynamics of the model in the domain $\Re^7_+$. In this region, the model can be considered has be mathematically and epidemiologically well posed showing that the total population of the model is bounded and is a unique solution representing a feasible problem[8].

2.3. Positivity and Boundedness

In this section of the model, it is said to be bounded and represent a unique solution i.e., the applicability to study physical systems is feasible.

Consider the compartmental disposition

$$\Pi = \left\{S(t), E(t), I(t), M(t), R(t), V(t) : N(t)\frac{\Lambda}{\mu} \in \Re^7_+\right\}.$$

It is obtained that each compartment of the model is deduced as follows;

$$\begin{aligned}
\frac{dS}{dt} &= \Lambda + (1-p)\Lambda + \delta R - \lambda(t)S - (\mu+\eta)S \Rightarrow \frac{dS}{dt} \geq -S(t)[\lambda(t) - (\mu+\eta)] \\
\frac{dS}{S(t)} &\geq -[\lambda(t) - (\mu+\eta)]dt \\
\int\frac{dS}{S(t)} &\geq -\int[\lambda(t) - (\mu+\eta)]dt \Rightarrow S(t) \geq S_0 e^{-\ell_0^t[\lambda(t)-(\mu+\eta)]t} > 0 \quad \text{At } t > 0, S(t) > 0
\end{aligned} \tag{2.5}$$

In the second compartment as deduced from the disease free equilibrium, it is obtained for $E(t)$, $I(t)$ and $R(t)$;

$$\begin{aligned} E^1 &= \lambda(t)S + \eta S - (\mu+\sigma)E, \quad \frac{dE}{dt} \geq -(\mu+\sigma)E(t), \\ \frac{dE}{E(t)} &\geq -(\mu+\sigma)dt, \Rightarrow \int \frac{dE}{E(t)} \geq -\int (\mu+\sigma)dt \\ E(t) &\geq E_0 \ell^{-(\mu+\sigma)t} > 0,\ t > 0,\ E(t) > 0 \end{aligned}$$

Subsequently this obtained for other compartments of the model equation 2.2 that;

$$\begin{aligned} I(t) \geq I_0 e^{-(\mu+\tau+\kappa\phi_1)t} > 0, \quad M(t) \geq I_0 e^{-(\mu+\omega)t} > 0, \\ R(t) \geq R_0 e^{-(\delta+\mu)t} > 0, \quad V(t) \geq R_0 e^{-(\mu_v+\gamma_v)t} > 0, \end{aligned} \tag{2.6}$$

Equation 2.5 and 2.6 above shows that equation 2.2 is in the positive quadrant of $\Re^7_+$, persisting in the attracting subset Π, which is compact, positively invariant and influential to the model. This portends with a well posed epidemiological and mathematically representing a solution to a physical problem.

2.4. Disease Free Equilibrium

This section discusses the equilibrium state of non-infected individuals with malaria spread which signifies a free states of health, encompassing individuals categorized as disease free states. Therefore, the total population is considered at equilibrium and the infected population are all subjected to zero.

$$\begin{aligned} 0 &= \Lambda + (1-p)\Lambda + \delta R - \lambda(t)S - (\mu+\eta)S \\ 0 &= \lambda(t)S + \eta S - (\mu+\sigma)E \\ 0 &= \sigma E - (\mu+\tau+\kappa\phi_1)I \\ 0 &= p\Lambda + (\tau+\kappa\phi_1)I - (\mu+\omega)M \\ 0 &= \omega M - (\delta+\mu)R \\ 0 &= \varphi_v - (\mu_v+\gamma_v)V + \alpha(1-\chi_2\phi_2)I \end{aligned}$$

When there is no progression of malaria fever, the disease population are at $t = 0$, where, $M_0 = \frac{p\Lambda}{(\omega+\mu)}$. Thus, the disease-free equilibrium when state variables of $E = I = 0$ yields:

$$(S, E, I, M, R, V) = \begin{pmatrix} S_0 = \dfrac{\Lambda + (1-p)\Lambda}{(\eta+\mu)} + \dfrac{\delta\omega pA}{(\eta+\mu)(\omega+\mu)(\delta+\mu)}, \\ E_0 = 0, \quad I_0 = 0, \quad M_0 = \dfrac{pA}{\mu+\omega}, \\ R_0 = \dfrac{\omega pA}{(\mu+\omega)(\delta+\mu)}, \quad V_0 = \dfrac{\varphi_v}{\mu_v+\gamma_v} \end{pmatrix} \tag{2.7}$$

2.5. Endemic Equilibrium Point

The dynamic nature of malaria prevalence, especially its central role in sustaining outbreaks within a population. To analyse the system at equilibrium, consider the set of equation (2), where the equilibrium points represent the endemic states of malaria prevalence. Let Ψ =

$(S^*, E^*, I^*, M^*, R^*, V^*)$ and $t > 0$, disease endemicity where $E^*, I^* > 0$. Each state variables are resolved in respect of their respective parameters where perseverance of malaria spread is noticed. Hence, it is obtained that the endemic equilibrium state for equation 2.2 is depicted below in equation 2.8.

$$\begin{aligned} S^* &= \frac{\Lambda + (1-p)\Lambda + \delta R^*}{\lambda^* + \mu + \eta}, \\ E^* &= \frac{\mu + \tau + \kappa\phi_1 I^*}{\sigma}, \\ R^* &= \frac{\omega[pA + (\tau + \kappa\phi_1)I^*]}{(\mu+\omega)(\delta+\mu)}, \\ M^* &= \frac{p\Lambda + (\tau + \kappa\phi_1)I^*}{\mu + \omega}, \\ V^* &= \frac{\varphi_v + \alpha(1-\chi_2\phi_2)I^*}{\mu_v + \gamma_v} \end{aligned} \tag{2.8}$$

2.6. Basic Reproduction Number

The measure of the potential new malaria progression observed from an infected individual in a population with no prior treatment within the system and to determine this, the next generation matrix method which focuses on the infectious classes of individuals and is resolved for the basic reproduction number [9]. This involves calculating the F and V matrices which represents the rates of new infections and transitions in and out of the infected compartments respectively. From the model equation 2.2, deriving these matrices as $G = F \times V^{-1}$ and ρ is the spectral radius of the matrix $|G - \lambda I|$. It is obtained from matrix F and V where R_* denotes the basic reproduction number.

$$\lambda = \frac{\beta(1-\chi_1\phi_2)V}{N_v}$$

$$f_i = \begin{pmatrix} (\lambda+\eta)S \\ \alpha(1-\chi_2\phi_2)I \end{pmatrix}, \qquad F_i = \begin{pmatrix} \frac{\beta(1-\chi_1\phi_2)S^*V}{N_v} \\ \alpha(1-\chi_2\phi_2)I \end{pmatrix},$$

$$F = \begin{pmatrix} 0 & 0 & \frac{\beta(1-\chi_1\phi_2)S^*V}{N_v} \\ 0 & 0 & 0 \\ 0 & \alpha(1-\chi_2\phi_2)I & 0 \end{pmatrix}$$

$V_i = \left(\frac{\partial v_i(x_i)}{\partial x_j}\right)$, at disease free equilibrium state, $v = \begin{pmatrix} (\sigma+\mu)E(t) \\ -\sigma E(t) + (\mu+\tau+\kappa+\phi_1)I(t) \\ (\mu_v+\gamma_v) \end{pmatrix}$

Then, the Jacobian of V is obtained as;

$$V = \begin{pmatrix} (\sigma+\mu) & 0 & 0 \\ -\sigma & (\mu+\tau+\kappa+\phi_1) & 0 \\ 0 & \alpha(1-\chi_2\phi_2) & (\mu_v+\gamma_v) \end{pmatrix}$$

Thus, the R_* is deduced from the relation that $R_* = FV^{-1}$ as

$$R_* = \frac{\beta\alpha\sigma(1-\chi_1\phi_2)(1-\chi_2\phi_2)S^*}{N_v(\mu+\sigma)(\mu+\tau+\kappa\phi_1)(\mu_v+\gamma_v)} \tag{2.9}$$

This determines the level of recovery rate and the spread of malaria disease. The leading eigenvalue of the non-invariant is the basic reproduction number of the disease model.

2.7. 2.7. Local Stability of Disease Free State

Local stability of the disease free equilibrium state for malaria fever was conducted by analysing the infectious population of (E, I and V). When the recurrence rate is less than unity it is asymptotically stable and if more than unity is unstable and the disease prevails. To deduce this disease-free equilibrium obtained as the Jacobian matrix of the system for equation (2) and this evaluated in equation (10) below.

$$J_{\ell_0} = \begin{pmatrix} -(\sigma+\mu) & 0 & \dfrac{\beta(1-\chi_1\phi_2)S}{N_v} \\ -\sigma & -(\mu+\tau+\kappa+\phi_1) & 0 \\ 0 & \alpha(1-\chi_2\phi_2) & -(\mu_v+\gamma_v) \end{pmatrix} \tag{2.10}$$

Respectively, the characteristic polynomial of equation 2.10, $|\lambda I - J_{E_0}| = 0$, which gives

$$(\lambda+\mu+\sigma)(\lambda+\mu+\tau+\kappa\phi_1)(\lambda+\mu_v+\gamma_v) - \frac{\beta\alpha\sigma(1-\chi_1\phi_2)(1-\chi_2\phi_2)S^*}{N_v} = 0,$$

from the result obtained in equation 2.10

$$(\lambda+\mu+\sigma)(\lambda+\mu+\tau+\kappa\phi_1)(\lambda+\mu_v+\gamma_v)(1-R_*) = 0.$$

All the eigenvalues satisfying equation 2.10 is less than zero if and only if $R_* < 1$, implying at equilibrium this is locally stable.

2.8. Local Stability of Endemic Equilibrium

Let the endemic equilibrium state be

$$\Delta = (S^*, E^*, I^*, M^*, R^*, V^*).$$

The Jacobian matrix evaluated Δ yields a full matrix. Due to the model is obtained that the local stability on the infected populations. The characteristic polynomial of equation 2.10 is obtained as

$$x^3 + a_1\lambda^2 + a_2\lambda + a_3 = 0. \tag{2.11}$$

The results obtained are equation 2.11 above where

$$\begin{aligned} a_1 &= (\mu+\sigma) + (\mu+\tau+\kappa\phi_1) + (\mu_v+\gamma_v), \\ a_2 &= (\mu+\sigma)(\lambda+\mu+\tau+\kappa\phi_1) + (\mu+\sigma)(\mu_v+\gamma_v) + (\mu+\tau+\kappa\phi_1)(\mu_v+\gamma_v), \\ a_3 &= (\mu+\sigma)(\mu+\tau+\kappa\phi_1)(\mu_v+\gamma_v)(R_*-1). \end{aligned}$$

Hence, for the local asymptotic stability using the Routh-Hurwitz condition, it requires that $a_1 > 0$, $a_3 > 0$ and $a_1a_2 > a_3$. Therefore, it is obtained that $a_1 > 0$ and $a_2 > 0$. Clearly, if $a_3 > 0 \Leftrightarrow R_* > 1$. Thus, the endemic equilibrium exists and is stable whenever $R_* > 1$.

2.9. Global Stability Analysis

This section, we employ the concept of Lyapunov function to establish the global asymptotic stability for the disease dynamics at equilibrium point. However, if $R_* < 1$ and unstable otherwise if $R_* > 1$ [10]. Therefore, via the concept of LaSalle's principle, consider the Lyapunov function;

$$L_0(E, I, V) = a_1 E + a_2 I + a_3 V$$

where $a_1, a_2, a_3 > 0$ are constants to be resolved for. Taking their derivatives with respect to time

$$\begin{aligned} L_0(E, I, V) &= a_1[\lambda S + \eta S - (\mu + \sigma)E] + a_2[\sigma E - (\mu + \tau + \kappa + \phi_1)I] \\ &\quad + a_3[\sigma_v - (\mu_v + \gamma_v) - a_2(\mu + \tau + \kappa\phi_1)]I \end{aligned}$$

evaluating at disease free equilibrium using $S \leq S^*$ we therefore obtain that,

$$\begin{aligned} L^* &\leq [a_1\beta(1 - \chi_1\phi_2)\frac{S^*}{N_v} - a_2(\mu_v + \gamma_v)V + [a_2\sigma - a_1(\mu + \sigma)]E \\ &\quad + [a_3\alpha(1 - \chi_2\phi_2) - a_2(\mu + \kappa + \kappa\phi_1)]I \end{aligned}$$

Choose

$$a_1 = \frac{\sigma}{\sigma + \mu}, \quad a_2 = 1, \quad a_3 = \frac{\beta(1 - \chi_1\phi_2)S^*}{N_v(\mu_v + \gamma_v)}.$$

The result of this yields in equation (2.12) below;

$$L^* \leq (\mu + \sigma)(\mu + \tau + \kappa\phi_1)(\mu_v + \gamma_v)(R_* - 1)I \tag{2.12}$$

From the above equation (2.12) at disease free equilibrium, $R_* < 1$, then $L^* < 0 \Leftrightarrow E = I = V = 0$. The LaSalle's invariance principle indicates that in the visible region, all trajectories converge to $L_* < 1$.

3. Numerical Simulation

In this section, we introduce some fundamental concepts relevant to the present study. We also outline the Laplace Adomian decomposition method and discuss the qualitative behaviour of the proposed mathematical model.

Definition 3.1. Let $\phi(t)$ be a sufficiently smooth function. The Laplace transform of its mth-order derivative is given by

$$L\left[\frac{d^m\phi(t)}{dt^m}\right] = s^m\Phi(s) - s^{m-1}\phi(0), \ldots, \phi^{(m-1)}(0) \tag{3.13}$$

where $\Phi(s) = L[\phi(t)]$.

Definition 3.2. Suppose an unknown function $U(t)$ can be expressed as an infinite series

$$U(t) = \sum_{k=0}^{\infty} U_k(t)$$

The Adomian polynomials $A_1, A_2, A_3, \ldots, A_n$ associated with a nonlinear operator $N(U)$ are defined by

$$A_n = \frac{1}{n!}\frac{d^n}{d\lambda^n}\left[N\left(\sum_{k=0}^{\infty} U_k\lambda^k\right)\right]_{\lambda=0}, \qquad n \geq 0 \tag{3.14}$$

Definition 3.3. Let (x_n) be a sequence and define the partial sums by

$$S_n = \sum_{k=1}^{n} x_k$$

The infinite series $\sum_{k=1}^{\infty} x_k$ is said to be convergent if the sequence (S_n) converges, that is,

$$\lim_{n\to\infty} S_n = S$$

Where S is a finite constant.

3.1. Laplace-Adomian Decomposition Method

Consider a general nonlinear ordinary differential equation of the form

$$\frac{d^m x(t)}{dt^m} = f(t, x(t)) \tag{3.15}$$

where $x(t)$ is the unknown function, $m \in N$ denotes the order of the differential equation, and $f(t, x(t))$ is a given nonlinear function. To implement the Laplace–Adomian decomposition method, we first apply the Laplace transform to both sides of 2.6, yielding

$$L\left[\frac{d^m x(t)}{dt^m}\right] = L[f(t, x(t))] \tag{3.16}$$

Using Definition 3.1, Eq. (3.13) becomes

$$s^m X(s) - s^{m-1}x(0), \ldots, x^{m-1}(0) = L[f(t, x(t))] \tag{3.17}$$

where $X(s) = L[x(t)]$. For simplicity, let $F(s) = L[f(t, x(t))]$. Then Eq. (3.14) can be written as

$$s^m X(s) - \sum_{k=0}^{m-1} s^{m-1-k} x^k(0) = F(s)$$

For the particular case $m = 1$, Eq. (3.17) reduces to $sX(s) - x(0) = F(s)$, which gives

$$X(s) = \frac{x(0)}{s} + \frac{1}{s}F(s)$$

Applying the inverse Laplace transform yields

$$x(t) = x_0(t) + L^{-1}\left[\frac{1}{s}F(s)\right]$$

where $x_0(t) = x(0)$ represents the initial approximation. The solution $x(t)$ is expressed as an infinite series

$$x(t) = \sum_{n=0}^{\infty} x_n(t)$$

Following Definition 3.2, the nonlinear term $f(t, x(t))$ is decomposed into a series of Adomian polynomials,

$$f(t, x(t)) = \sum_{n=0}^{\infty} A_n(t). \tag{3.18}$$

where the Adomian polynomials A_n are defined by

$$A_n = \frac{1}{n!}\frac{d^n}{d\lambda^n}\left[f\left(t, \sum_{k=0}^{\infty} x_k(t)\lambda^k\right)\right]_{\lambda=0}, \; n \geq 0$$

Substituting Eq. (3.13) and (3.17) into Eq. (3.18) yields the recursive scheme

$$x_{n+1}(t) = L^{-1}\left[\frac{1}{s}L(A_n(t))\right], \; n \geq 0$$

The approximate solution of order N is therefore given by

$$x(t) \approx \sum_{n=0}^{N} x_n(t)$$

According to Definition 3.3, the series solution (3.14) is convergent if

$$\lim_{x\to\infty} x_n(t) = 0 \tag{3.19}$$

in which case $\sum_{n=0}^{\infty} x_n(t)$ converges to the exact solution $x(t)$.

$$\begin{aligned}
L[S^1] &= L[\Lambda + (1-p)A + \delta R] - L[\lambda(t)S - (\mu+\eta)S] \\
L[E^1] &= L[\lambda(t)S + \eta S] - L[(\mu+\sigma)E] \\
L[I^1] &= L[\sigma E] - L[(\mu+\tau+\kappa\phi_1)I] \\
L[M^1] &= L[pA + (\tau+\kappa\phi_1)I] - L[(\mu+\omega)M] \\
L[R^1] &= L[\omega M] - L[(\delta+\mu)R] \\
L[V^1] &= L[\varphi_v] - L[(\mu+\gamma_v)V + \alpha(1-\chi_2\phi_2)I]
\end{aligned} \tag{3.20}$$

Evaluate from equation (3.20) above to yield equation (21) below,

$$\begin{aligned}
mL[S] &= S(0) + L[\Lambda + (1-p)A + \delta R] - L[\lambda(t)S - (\mu+\eta)S] \\
mL[E] &= E(0) + L[\lambda(t)S + \eta S] - L[(\mu+\sigma)E] \\
mL[I] &= I(0) + L[\sigma E] - L[(\mu+\tau+\kappa\phi_1)I] \\
mL[M] &= M(0) + L[pA + (\tau+\kappa\phi_1)I] - L[(\mu+\omega)M] \\
mL[R] &= R(0) + L[\omega M] - L[(\delta+\mu)R] \\
mL[V] &= V(0) + L[\varphi_1] - L[(\mu+\gamma_v)V + \alpha(1-\chi_2\phi_2)I]
\end{aligned} \tag{3.21}$$

when $S(0) = s_0,\ E(0) = e_0,\ I(0) = i_0,\ M(0) = m_0,\ R(0) = R_*$ and $V(0) = v_0$

$$\begin{aligned}
L[S(t)] &= s_0 + \frac{L}{m}[\Lambda + (1-p)A + \delta R] - L[\lambda(t)S - (\mu+\eta)S] \\
L[E(t)] &= e_0 + \frac{L}{m}[\lambda(t)S + \eta S] - [(\mu+\sigma)E] \\
L[I(t)] &= i_0 + \frac{L}{m}[\sigma E] - [(\mu+\tau+\kappa\phi_1)I] \\
L[M(t)] &= m_0 + \frac{L}{m}[pA + (\tau+\kappa\phi_1)I] - [(\mu+\omega)M] \\
L[R(t)] &= R_* + \frac{L}{m}[\omega M] - [(\delta+\mu)R] \\
L[V(t)] &= s_0 + \frac{L}{m}[\varphi_v] - [(\mu_v+\gamma_v)V + \alpha(1-\chi_2\phi_2)I]
\end{aligned} \tag{3.22}$$

Deduce for the non-linear terms in the iteration equation (3.22) above and substitutes by taking the inverse Laplace transform of both sides to obtain equation (3.23) below.

$$\begin{aligned}
S(t) &= s_0 + L^{-1}\left[\frac{1}{m}\left[\Lambda + (1-p)A + \delta R\right] - L[\lambda(t)S - (\mu+\eta)S]\right] \\
E(t) &= e_0 + L^{-1}\left[\frac{1}{m}\left[\lambda(t)S + \eta S\right] - L[(\mu+\sigma)E]\right] \\
I(t) &= i_0 + L^{-1}\left[\frac{1}{m}\left[\sigma E\right] - L[(\mu+\tau+\kappa\phi_1)I]\right] \\
M(t) &= m_0 + L^{-1}\left[\frac{L}{m}\left[pA + (\tau+\kappa\phi_1)I\right] - L[(\mu+\omega)M]\right] \\
R(t) &= R_* + L^{-1}\left[\frac{L}{m}\left[\omega M\right] - L[(\delta+\mu)R]\right] \\
V(t) &= s_0 + L^{-1}\left[\frac{L}{m}\left[\varphi_v\right] - L[(\mu_v+\gamma_v)V + \alpha(1-\chi_2\phi_2)I]\right]
\end{aligned} \tag{3.23}$$

Subsequently, iteration result obtained from the above equation (3.22) yields;

$$\begin{aligned}
\sum_{n=0}^{\infty} S_n(t) &= s_0 + L^{-1}\left[\frac{1}{m}[\Lambda + (1-p)A + \delta\sum_{n=0}^{\infty} R_n - [\lambda(t)\sum_{n=0}^{\infty} S_n - (\mu+\eta)\sum_{n=0}^{\infty} S_n]\right] \\
\sum_{n=0}^{\infty} E_n(t) &= e_0 + L^{-1}\left[\frac{1}{m}[\lambda(t)\sum_{n=0}^{\infty} S_n + \eta\sum_{n=0}^{\infty} S_n - ((\mu+\sigma)\sum_{n=0}^{\infty} E_n)]\right] \\
\sum_{n=0}^{\infty} I_n(t) &= i_0 + \frac{L}{m}\left[[\sigma\sum_{n=0}^{\infty} E_n - ((\mu+\tau+\kappa\phi_1)\sum_{n=0}^{\infty} I_n)]\right] \\
\sum_{n=0}^{\infty} M_n(t) &= m_0 + L^{-1}\left[\frac{1}{m}[pA + (\tau+\kappa\phi_1)\sum_{n=0}^{\infty} I_n - ((\mu+\omega)\sum_{n=0}^{\infty} M_n)]\right] \\
\sum_{n=0}^{\infty} R_n(t) &= R_* + L^{-1}\left[\frac{1}{m}[\omega\sum_{n=0}^{\infty} M_n - ((\delta+\mu)\sum_{n=0}^{\infty} R_n)]\right] \\
\sum_{n=0}^{\infty} V_n(t) &= s_0 + L^{-1}\left[\frac{1}{m}[\varphi_v - ((\mu_v+\gamma_v)\sum_{n=0}^{\infty} V_n + \alpha(1-\chi_2\phi_2)\sum_{n=0}^{\infty} I_n)]\right]
\end{aligned}$$

The initial approximations of each class are given by equation (3.21), comparing the coefficients at $n = 1, 2, 3....$ Using the recurrence relations obtained from the iteration results. Further iterations are done to obtain successive iterative terms at $n = 2$.

$$\begin{aligned}
S_2(t) &= (ps_0 + \alpha is_0 + \alpha is_0\mu_0 - \alpha is_0\rho_0 - \alpha is_0e_0 + \alpha is_0\beta_1 + \alpha is_0\eta)t^2 \\
&\quad -(\mu^2 s_0 + \kappa\mu s_0 + \tau\mu v_0 - \delta s_0 + \phi_{12}s_0 + \omega v_0 + \phi_1 s_0)t \\
E_2(t) &= (\alpha is_0\xi_2 + \mu^2 v_0 - \gamma_v\mu s_0 + \phi_1\mu s_0 + \varphi s_0 + \eta v_0 + \phi^2 v_0)t^2 + (\alpha i_0\rho t - \eta\mu\omega - \omega e_0 + \omega s_0\eta)t \\
I_2(t) &= (\alpha i_0\omega + \alpha i_0\mu - \alpha i_0\omega + \alpha e_0\omega_1 + \mu^2 p - \alpha i_0\omega\gamma_1)t^2 + (\alpha^2 i^2 s_0 - Ais_0 + \alpha is_0\mu_0 + \alpha is_0\omega_0 \\
&\quad -\Lambda is_0b_0 - \mu^2 ie_0\omega + \alpha ie_0\omega^2)t \\
M_2(t) &= (\alpha i_0\gamma + \sigma i_0\Phi\mu - \alpha i_0\omega + \alpha e_0\eta_1 - \mu^2\chi_2 + \alpha i_0\omega_1)t^2 + (\alpha is_0\mu_0 - \alpha is_0 + \alpha is_0\gamma v_0 \\
&\quad -\tau^2 ie_0\eta + \alpha ie_0\delta^2)t \\
R_2(t) &= (\alpha is_0 + \gamma^2 i_0 + \delta\mu i_0 + \chi_2\sigma ie_0 + \mu^2 i_0 - \mu\omega i_0)t^2 - (\omega^2 i_0 - \phi\sigma ie_0 - pe_0)t \\
V_2(t) &= (\alpha i_0\gamma_v + \alpha i_0\mu - \alpha i_0\omega - \alpha e_0\eta_1 - \chi_2\phi_2 + \alpha i_0\omega_1)t^2 + (\alpha is_0\gamma_v - \mu^2 e_0\eta + \alpha ie_0)t
\end{aligned} \tag{3.24}$$

Iterations can be carried on. This can be furthered till the desired results expected are obtained. Thus, as obtained the raw solution to each model compartment is summarized as we have it in equation (3.25) below.

$$\begin{aligned} S(t) &= \sum_{k=0}^{3} s_k(t), \quad E(t) = \sum_{k=0}^{3} e_k(t), \quad I(t) = \sum_{k=0}^{3} i_k(t), \\ M(t) &= \sum_{k=0}^{3} m_k(t), \quad R(t) = \sum_{k=0}^{3} r_k(t), \quad V(t) = \sum_{k=0}^{3} v_k(t). \end{aligned} \tag{3.25}$$

Evaluating these series results using the corresponding variables and parameter values for the iterative terms of (3.24), it is therefore obtained in equation (3.26) below;

$$\begin{aligned} S(t) &= 1000.2 - 1.293t + 1.263263t^3 \\ E(t) &= 0.01591.4t + 0.1376t^2 - 1.2773t^3 \\ I(t) &= 0.273 + 1.109t + 2.95t^2 + 1.9345t^3 \\ M(t) &= 11 - 1.72t - 1.982t^2 + 0.009t^3 \\ R(t) &= 1.42 + 9.60t + 0.008t^2 - 0.26t^3 \\ V(t) &= 1.020 - 0.73t - 0.661t^2 + 1.254t^3 \end{aligned} \tag{3.26}$$

3.2. Results

Results obtained from the numerical simulation was interpreted pictorially in relation to the control mechanisms considered for the mitigation of malaria progression as seen in the Figures 1 to 5 below.

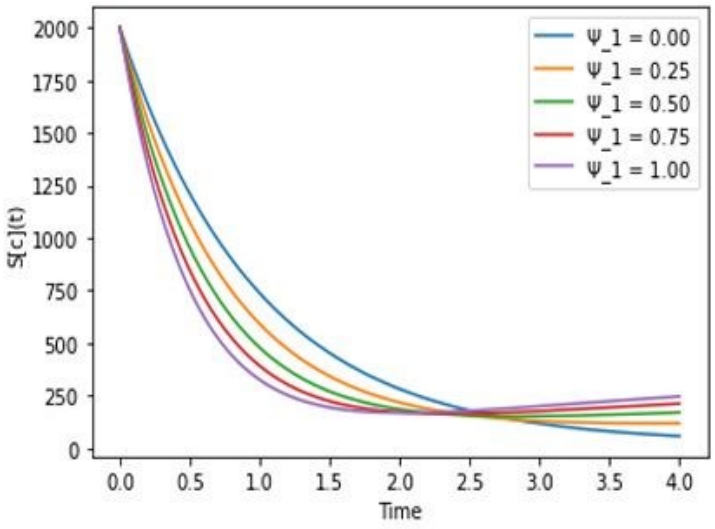

Figure 3.1: Increased use of mint leaf therapy may enhance immune response and provide mild antimalarial effects, lowering parasite density in infants. Combined with proper environmental sanitation to reduce mosquito breeding, it significantly decreases malaria transmission and infection rates.

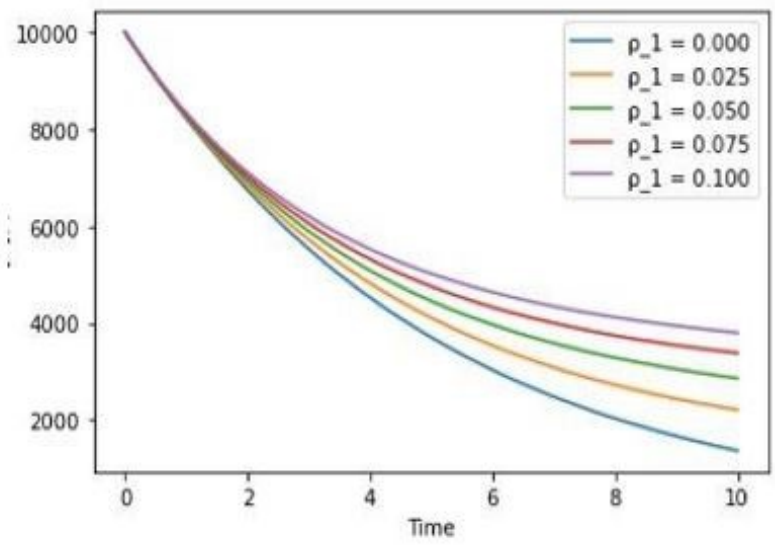

Figure 3.2: Improved environmental sanitation eliminates stagnant water and waste that serve as mosquito breeding sites. This reduces mosquito population density and human–vector contact, lowering malaria transmission risk. When combined with mint leaf therapy, it enhances overall malaria control among infants

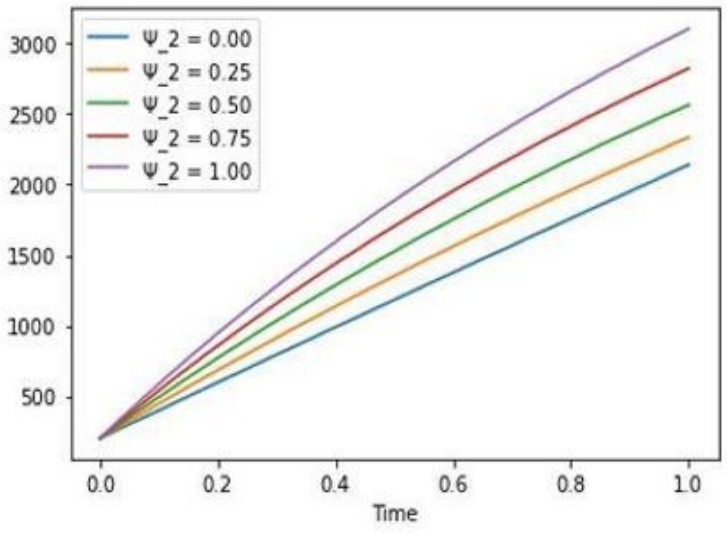

Figure 3.3: Combining mint leaf therapy with improved sanitation provides dual protection: mint leaf reduces parasite load in infected infants, while sanitation lowers mosquito breeding and exposure. This integrated approach significantly decreases malaria transmission and overall disease prevalence.

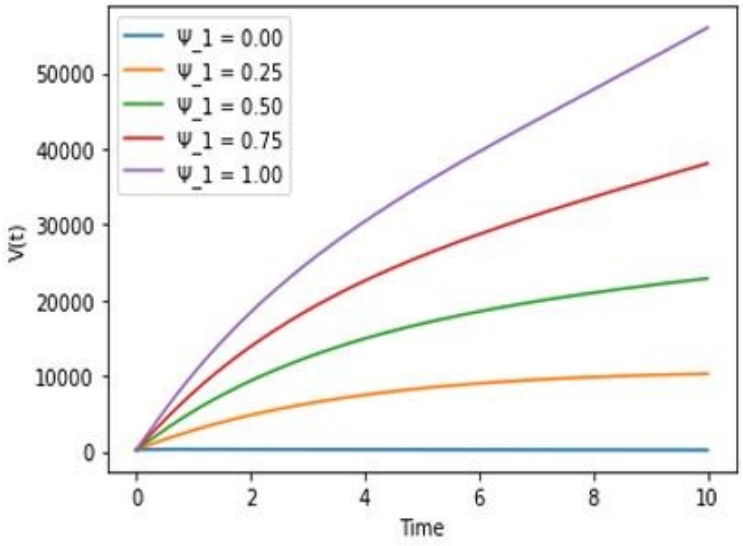

Figure 3.4: Higher control intensity through consistent mint leaf therapy and strict environmental sanitation rapidly reduces parasite transmission and mosquito density. This accelerates decline in infection cases, enabling the population to stabilize more quickly toward malaria elimination.

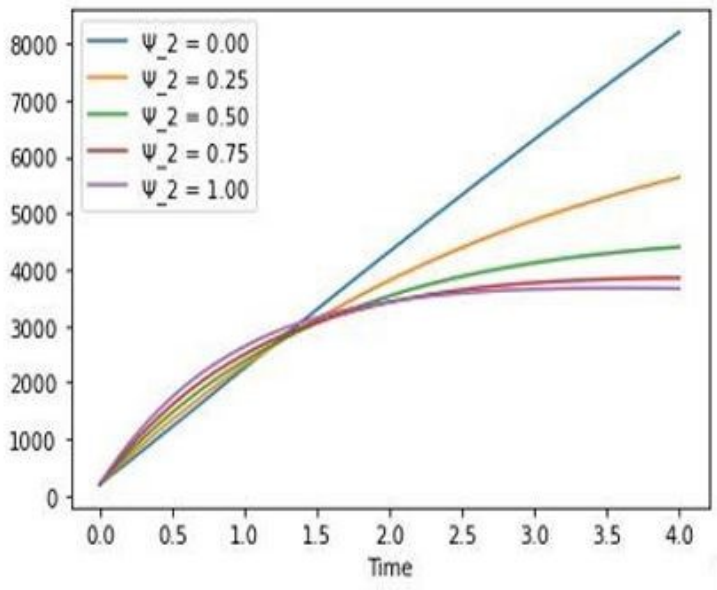

Figure 3.5: Sustained environmental sanitation continuously removes mosquito breeding sites, maintaining low vector density and reducing reinfection risk. When maintained alongside mint leaf therapy, it prevents resurgence and supports long-term malaria control and stability.

4. Discussion of results

The malaria dynamics was studied over time whose simulation results were intercepted using the Maple software tool, with the outputs presented in Figures 3.1 to 3.5. These figures provide

crucial insights into the impact of treatment and public awareness strategies through sanitation on the control of malaria fever within a population. Figure 3.1, its shows the effect of mint leaf therapy with a noticeable decline in the infected infant population as the mint-leaf therapy control increases, indicating its effectiveness in reducing malaria parasite load and shortening the infectious period. Figure 3.2, indicates the role of environmental sanitation. Improved sanitation levels lead to a steady reduction in mosquito population density which is reflected in a lower force of infection among infants over time. Figure 3.3, helps with the combined control measures whose results demonstrate that the simultaneous application of mint leaf therapy and sanitation produces a stronger reduction in malaria transmission than either control applied alone. Figure 3.4, the sensitivity to Control Intensity the plots reveal that higher intensity of mint leaf therapy coverage results in faster stabilization of the system toward a malaria-free equilibrium. Figure 3.5, shows that in long-term consideration the transmission dynamics and time-series indicate that sustained sanitation efforts significantly suppress malaria resurgence, maintaining low infection levels even after initial treatment effects decline.

5. Conclusion

This study successfully employed the Laplace Adomian decomposition method to derive numerical solution for assessing the impact of high treatment and sanitation on malaria fever. The approach demonstrated strong effectiveness, significantly reducing the basic reproduction number below unity which is a crucial threshold for disease control. Through numerical simulation results, the influence of varying sanitation and treatment rates on malaria mitigation within the population was examined. Detailed behavioural analysis of the population responses over time, supported by graphical illustrations, revealed key epidemiological patterns and biological insights. Importantly, the findings underscore the crucial role of combining treatment efforts with improved environmental sanitation in preventing the spread of malaria disease. These measures serve as an essential components in developing sustainable measures for disease containment and eventual eradication. However, the implementation of awareness campaigns and health education programs remains vital to prone water logged communities within suburb of African communities. Behavioural interventions, when integrated into public health safety measures will enhance the long-term effectiveness of biomedical control strategies. This multifaceted approach that includes both medical and behavioural components to combat malaria spread will be of long term effectiveness.

Funding

No funding was received.

Conflict of Interest

Authors declare no conflict of interest

Data Availability Statement

Data sets generated during this research are available from the corresponding author upon request.

Acknowledgement

Authors acknowledged efforts of all members of Staff in the Department of Mathematical Sciences, Osun State University, Osogbo, Nigeria, towards the success of this research.

References

[1] C. Boudin, M. Olivier, J. F. Molez, J. P. Chiron, and P. Ambroise-Thomas, "High human malarial infectivity to laboratory-bred anopheles gambiae in a village in burkina faso," *American Journal of Tropical Medicine and Hygiene*, vol. 48, no. 5, pp. 700–706, 1993. View online.

[2] N. J. White, D. Chapman, and G. Watt, "The effects of multiplication and synchronicity on the vascular distribution of parasites in falciparum malaria," *Transactions of the Royal Society of Tropical Medicine and Hygiene*, vol. 86, no. 6, pp. 590–597, 1992. View online.

[3] Z. A. Jeremiah and E. K. Uko, "Depression of platelet counts in apparently healthy children with asymptomatic malaria infection in a nigerian metropolitan city," *Platelets*, vol. 18, pp. 469–471, 2007. View online.

[4] F. Robert, F. Ntoumi, G. Angel, D. Candito, C. Rogier, T. Fandeur, J. L. Sarthou, and O. Mercereau-Puijalon, "Extensive genetic diversity of plasmodium falciparum isolates collected from patients with severe malaria in dakar, senegal," *Transactions of the Royal Society of Tropical Medicine and Hygiene*, vol. 90, pp. 704–711, 2023. View online.

[5] M. K. Kolawole and K. A. Odeyemi, "Behavioural analysis of seirm-based optimal control strategies for cholera in endemic regions of west africa," *Adeleke University Journal of Science (AUJS)*, vol. 4, no. 2, pp. 495–523, 2025. View online.

[6] F. Vidal, J. C. Vidal, A. P. R. Gadelha, C. S. Lopes, M. G. P. Coelho, and L. H. Monteiro, "The effects of extracts and fractions from mentha x piperita lin. (lamiaceae) on trophozoites," *Experimental Parasitology*, vol. 115, pp. 25–31, 2007. View online.

[7] M. A. Ansari, P. Vasudevan, M. Tandon, and R. K. Razdan, "Larvicidal and mosquito repellent action of peppermint (mentha piperita) oil," *Bioresource Technology*, vol. 7, no. 1, pp. 267–271, 2024. View online.

[8] G. Buppesh, C. Amutha, S. Nandagopal, A. Ganeshkumar, P. Sureshkumar, and K. S. Murali, "Antibacterial activity of mentha piperita l. (peppermint) from leaf extracts – a medicinal plant," *Acta Agriculturae Slovenica*, vol. 1, no. 9, pp. 73–79, 2023. View online.

[9] A. Coppi, M. Cabinian, D. Mirelman, and P. Sinnis, "Antimalarial activity of allicin, a biologically active compound from garlic cloves," *Antimicrobial Agents and Chemotherapy*, vol. 50, no. 5, pp. 31–47, 2005. View online.

[10] K. A. Odeyemi and M. K. Kolawole, "Stability analysis of sveitr model for cholera control with treatment and vaccination using laplace adomian decomposition method," *Jurnal Diferensial*, vol. 7, no. 1, pp. 85–105, 2025. View online.

Citation IEEE Format:
B. O. Awominure, A. O. Popoola, and T. Oreyeni. *"Modeling the Impact of Mint Leaf Therapy and Sanitation on Malaria Transmission among Infants"*, *Jurnal Diferensial*, vol. 8(2), pp. 120-135, 2026.